

Dual Space Minimum Information Entropy Sum In A High Frequency Periodic Driving Of Quantum Systems

Deep Raj Meena

A dissertation submitted for the partial fulfillment of
BS-MS dual degree in Science



**INDIAN INSTITUTE OF SCIENCE EDUCATION AND
RESEARCH, MOHALI**

April 2015

Certificate of Examination

This is to certify that the dissertation titled **Dual Space Minimum Information Entropy Sum In High Frequency Periodic Driving Of Quantum Systems** submitted by **Mr. Deep Raj Meena (Reg. No. MS09044)** for the partial fulfilment of BS-MS dual degree programme of the Institute, has been examined by the thesis committee duly appointed by the Institute. The committee finds the work done by the candidate satisfactory and recommends that the report be accepted.

Dr. Arijit Kumar De

Dr. K. P. Yogendran

Dr. P. Balanarayan
(Supervisor)

Dated: April 24, 2015

Declaration

The work presented in this dissertation has been carried out by me with Dr. P. Balanarayan at the Indian Institute of Science Education and Research Mohali. This work has not been submitted in part or in full for a degree, a diploma, or a fellowship to any other university or institute. Whenever contributions of others are involved, every effort is made to indicate this clearly, with due acknowledgement of collaborative research and discussions. This thesis is a bonafide record of original work done by me and all sources listed within have been detailed in the bibliography

Deep Raj Meena
(Candidate)

Dated: April 24, 2015

In my capacity as the supervisor of the candidates project work, I certify that the above statements by the candidate are true to the best of my knowledge.

Dr. P. Balanarayan
(Supervisor)

“All characters appearing in this work are fictitious. Any resemblance to any sort of realism, is purely coincidental.”

Acknowledgements

I would like to express my special appreciation and thanks to my advisor Dr. P. Balanarayan, you have been a good mentor for me. I would like to thank you for encouraging my research and for allowing me to develop problem solving skills independently. Your advice on both research as well as on my career have been priceless. I would also like to thank Dr Arijit Kumar De and Dr K. P. Yogendran for serving as my committee members. I would also acknowledge head of department Professor K. S. Viswanathan for his quick resolution of issues. The Inspire programme and IISER Mohali are equally acknowledged.

A special thanks to my family. Words cannot express how grateful I am to my mother, and father for all of the sacrifices that you have made on my behalf. Your prayer for me was what sustained me thus far. I would also like to acknowledge some of my very close friends Anuj, Bharat, Jugal, Nishant, Neeraj, Prateek.

Later in the journey Ashish Thakur and Pankaj The Dubey joined and are very much part of fun. I would further like to thank Neeraj Sangwan who always kept on asking me *Thesis done?* and pushed me to write it. Remembering all those sleepless nights, the moments when there was no one to answer my queries always cheer me up.

Deep Raj Meena

Contents

| | |
|---|------------|
| Acknowledgements | iv |
| List of Figures | vii |
| Abbreviations | ix |
| Abstract | xi |
| 1 Introduction | 1 |
| 1.1 Preamble | 1 |
| 1.2 Electron density in position space | 2 |
| 1.3 Electron density in momentum space ^[12] | 3 |
| 1.4 Information Entropies | 4 |
| 1.5 Generalized uncertainty relations | 6 |
| 1.6 High Frequency AC fields | 8 |
| 1.7 Kramer-Henneberger transformation | 9 |
| 1.8 Motivation and plan of thesis | 10 |
| REFERENCES | 10 |
| 2 Program for Electron Density and Electron Momentum Density | 13 |
| 2.1 Introduction | 13 |
| 2.2 Electronic structure calculation | 14 |
| 2.3 ED and EMD Code description | 16 |
| 2.3.1 Primitives | 16 |
| 2.3.2 Contraction level normalization | 17 |
| 2.4 Results | 19 |
| REFERENCES | 21 |
| 3 Model Problems | 22 |
| 3.1 Harmonic Oscillator | 22 |

| | | |
|-------------------|--|-----------|
| 3.1.1 | Case 1 : $\sigma > 1$ | 23 |
| 3.1.2 | Case 2 : $\sigma < 1$ | 24 |
| 3.1.3 | Case 3 : $\sigma = 1$ | 25 |
| 3.1.4 | KH Transformation on a harmonic oscillator potential | 26 |
| 3.1.5 | Minimum Information Entropy Driving | 30 |
| 3.2 | MORSE POTENTIAL | 32 |
| 3.3 | XENON POTENTIAL | 37 |
| REFERENCES | | 41 |

List of Figures

| | | | |
|------|--|--|----|
| 1.1 | (a) <i>blue</i> : $ \Psi(x) ^2$ | (b) <i>black</i> : $ \Psi(p) ^2$ | 5 |
| 1.2 | (a) $V(x)$ (<i>in black</i>) | (b) $V_{0\ KH}$ (<i>in blue</i>)(effective non-ionizing potential for an atom) | 8 |
| 2.1 | Helium in position space at $Z = 0$ (<i>a.u.</i>). | | 19 |
| 2.2 | Helium in position space at $Y = Z = 0.0$ (<i>a.u.</i>) | | 19 |
| 2.3 | Helium in momentum space at $P_Z = 0$ (<i>a.u.</i>). | | 20 |
| 2.4 | Helium in momentum space at $P_Y = P_Z = 0.0$ (<i>a.u.</i>) | | 20 |
| 3.1 | Probability densities in position and momentum space for $\sigma > 1$. | | 23 |
| 3.2 | Information entropies in position and momentum space as a function of vibrational state for $\sigma > 1$. | | 24 |
| 3.3 | Probability densities in position and momentum space for $\sigma < 1$. | | 24 |
| 3.4 | Information entropies in position and momentum space as a function of vibrational state for $\sigma < 1$. | | 25 |
| 3.5 | Probability densities in position and momentum space for $\sigma = 1$. | | 25 |
| 3.6 | Information entropies in position and momentum space as a function of vibrational state for $\sigma = 1$ in which there is an equal distribution in position and momentum space. | | 26 |
| 3.7 | Ground state driving of V_{KH} (in blue) of harmonic Oscillator to 5^{th} and 10^{th} excited state of previous $V(x)$ (in Red) under Kh Transformation. | | 31 |
| 3.8 | Morse potential for hydrogen molecule as a function of α_0 . | | 33 |
| 3.9 | Energy levels for morse potential for hydrogen molecule. | | 34 |
| 3.10 | State Energies for morse potential for hydrogen molecule as a function of α_0 . | | 34 |
| 3.11 | Morse potential for hydrogen molecule and Probability densities for Ground state in position space as function of α_0 | | 35 |
| 3.12 | Morse potential for hydrogen molecule and Probability densities for First excited state in position space as function of α_0 | | 35 |
| 3.13 | The corresponding Probability densities for Ground state in momentum space as function of α_0 | | 35 |
| 3.14 | The corresponding Probability densities for First excited state in momentum space as function of α_0 | | 35 |
| 3.15 | Ground state Information entropies as a function of α_0 | | 36 |
| 3.16 | First excited state Information entropies as a function of α_0 | | 36 |

| | | |
|------|---|----|
| 3.17 | Energy levels for xenon model potential depicting two perfectly bound states. | 38 |
| 3.18 | The two bound states Energies for xenon model potential as a function of α_0 | 38 |
| 3.19 | Xenon model potential and Probability densities for Ground state in position space as function of α_0 | 39 |
| 3.20 | Xenon model potential and Probability densities for First excited state in position space as function of α_0 | 39 |
| 3.21 | The corresponding Probability densities for Ground state in momentum space as function of α_0 | 39 |
| 3.22 | The corresponding Probability densities for First excited state in momentum space as function of α_0 | 39 |
| 3.23 | Ground state Information entropies as a function of α_0 | 40 |
| 3.24 | First excited state Information entropies as a function of α_0 | 40 |

Abbreviations

| | |
|-------------|---|
| a.u. | a tomic u nits |
| DVR | D iscrete V ariable R epresentation |
| ED | E lectron D ensity |
| EMD | E lectron M omentum D ensity |
| TDSE | T ime D ependent S chrödinger E quation |

*Dedicated to ... my Parents
and loving sister*

Abstract

A quantum system is associated with uncertainty in position and momentum space as given by the Heisenberg uncertainty principle, $\Delta x \Delta p_x \geq \hbar$. This unbreakable lower bound is made even more stronger by the information theoretic inequality, $S_\rho + S_\gamma \geq n(1 + \ln \pi)$ [I. Białynicki-Birula, and J. Mycielski, Comm. Math. Phys. 44, 2,(1975), 129-132.], where S_ρ and S_γ are information entropies due to the single particle charge densities in position and momentum spaces respectively. In this work, the question of how close to and in what fashion can this bound be achieved is addressed. It is numerically shown that this is possible *via* a high frequency AC driving of the quantum system. In the presence of high frequency AC fields instead of *ionization*, stabilization happens for certain field parameters. A minimum in the information entropy sum of dual spaces is numerically shown for model quantum systems under periodic high frequency driving conditions. The AC field parameters at which the information entropy sum is minimum, is given in terms of the classical quiver distance $\alpha_0 = \frac{\epsilon_0}{m_e \omega^2}$, where ϵ_0 , field strength and ω is the frequency.

A code has been developed for calculating electron momentum densities of atoms from the electronic wavefunctions calculated using the GAMESS(General Atomic and Molecular Electronic Structure System) package. From this information entropies in position/momentum space have been calculated for the ground state of closed shell atoms with fully filled orbitals.

Chapter 1

Introduction

1.1 Preamble

At a microscopic level, the quantum system can be described by a wave function. the wave function itself is not an experimentally measurable quantity. The probability density corresponding to the wave function is what can be experimentally measured. How would one extract the necessary chemical and physical information from the density has always been a problem of interest. In this sense, the information entropies are a useful tool to characterize the uncertainty in a quantum system in conjugate position and momentum spaces. Given the $4N$ -dimensional wave function for an N -particle system, one can condense the information that it carries, into a physically intuitive three dimensional form called the single particle charge density. Condensing the $6N$ -dimensional phase space density could amount to separately analyzing the behaviour of an N -particle system in position space and momentum space. It is of relevance that the resultant single particle densities are experimentally measurable. However, there is still a matter of the *natural* quantum uncertainty. To probe a quantum system, using high frequency and high intensity oscillating fields, has become a norm of the day. In this thesis, the information theoretic characterization of conjugate space densities of AC driven quantum systems is examined. In the forthcoming sections the analyzed quantities are defined and introduced. In the next section density distributions in dual spaces are described. [1].

1.2 Electron density in position space

A chemist has always been interested in the quantum mechanical elucidation of structure, which has an experimental realization through spectroscopic techniques. The single particle charge density that can be obtained from X-ray diffraction experiments gives the structure of a chemical system.

For an N -electron system, (discrete spins summed over),

$$\rho(\vec{r}) = N \sum_{\sigma} \int \Psi^*(\vec{r}, \vec{r}_2, \vec{r}_3, \dots, \vec{r}_N) \Psi(\vec{r}, \vec{r}_2, \vec{r}_3, \dots, \vec{r}_N) d^3r_2 d^3r_3 \dots d^3r_N \quad (1.1)$$

The N -particle wave function, Ψ , is normalized which implies that the charge density $\rho(\vec{r})$ integrates out to the total number of electrons N .

$$\int \rho(\vec{r}) d^3r = N \quad (1.2)$$

Given the molecular orbitals $\{\psi_a(\vec{r})\}$, the density is given by,

$$\rho(\vec{r}) = \sum_{a=1}^k |\psi_a(\vec{r})|^2 \quad (1.3)$$

Where k is number of filled orbitals. The atomic charge density possesses a finite maximum at the nuclear position. A spherical average of the charge density at a nuclear position satisfies Kato's [2] cusp condition [3–5].

$$\left. \frac{d\tilde{\rho}}{dr} \right|_{r=0} = -2Z\tilde{\rho}(0) \quad (1.4)$$

Here Z is the charge of the atomic nucleus and $\tilde{\rho}(r)$ is the spherically averaged charge density.

Asymptotically, the behaviour of the charge density is described by [6–9],

$$\left. \frac{\partial \ln[\tilde{\rho}(r)]}{\partial r} \right|_{r \rightarrow \infty} = -2\sqrt{2I} \quad (1.5)$$

where I is atomic ionization potential. The electron densities decay as e^{-2Zr} near the nucleus and $e^{-2r\sqrt{2I}}$ far away from the nucleus. The intermediate behaviour between cusp and the asymptotics can only be numerically observed for atomic densities [10, 11].

1.3 Electron density in momentum space [12]

The discussion of atoms and molecules in momentum space began with the work of Pauling and Podolsky [13] in 1929, where they applied a Fourier-Dirac transformation as given by Jordan [14] in 1927, to hydrogenic orbitals. Their aim was to obtain the wave function and thus the probability of an electron being in a given momentum range. This was also related to Compton line experiments giving the electron momentum density [15]. There is another technique involving the measurement of momentum densities called electron momentum spectroscopy (EMS) [16]. Most of work in chemistry on electron momentum density (EMD) has been due to Coulson [17–19].

The momentum space wave function is obtained by a Fourier transform of the position space wave function and is given by,

$$\Phi(\vec{p}_1, p_2, \dots, \vec{p}_N) = \frac{1}{(2\pi)^{3N/2}} \int d^3r_1 d^3r_2 \dots d^3r_N \Psi(\vec{r}_1, \vec{r}_2, \dots, \vec{r}_N) e^{-i \sum_{i=1}^N \vec{r}_i \cdot \vec{p}_i} \quad (1.6)$$

For an N -electron system, the momentum space density is,

$$\gamma(\vec{p}) = N \sum_{\sigma} \int \Phi^*(\vec{p}, \vec{p}_2, \vec{p}_3, \dots, \vec{p}_N) \Phi(\vec{p}, \vec{p}_2, \vec{p}_3, \dots, \vec{p}_N) d^3p_2 d^3p_3 d^3p_4 \dots d^3p_N \quad (1.7)$$

The EMD also has additional characteristics of being inversion symmetric i.e $\gamma(-\vec{p}) = \gamma(\vec{p})$ [20]. It has an asymptotic decay of p^{-8} in the far momentum range. The EMD for ground state of helium in momentum space shows monotonic behaviour. On the other hand, EMD for ground state of neon a has minimum at $p = 0$ and maximum at $p \approx 9.0$ a.u, and hence shows non-monotonicity. A nonmonotonic behaviour has been first noticed and recorded by Thakkar [21] for carbon, nitrogen, oxygen, fluorine, neon and argon atoms. The carbon, nitrogen,

oxygen and fluorine atoms were found to show at most three maxima in their spherically averaged momentum densities. Later, Koga et al. [22] classified the 103 elements of the periodic table with EMDs of three types: (i) monotonic, (ii) nonmonotonic, and (iii) those having 2 maxima, one at $p = 0$ and the other at $p > 0$. A characterization of the spread/localization/uncertainty in these distribution is done by information theoretic measures. The next section defines and introduces these.

1.4 Information Entropies

Since probabilities are fundamental at a microscopic level, the description of the system is more often represented in terms of uncertainty. Shannon [23] described uncertainty for a set of possible events in terms of information entropies for a discrete probability distribution as having following characteristics :

1. The quantity S should be continuous in P_i , where P_i is probability of i^{th} outcome.
2. If all P_i are equal, $P_i = \frac{1}{n}$, then the quantity S will be maximum and a monotonic increasing function of n .
3. If a choice is broken down into two successive choices, the original S should be a weighted sum of the individual values of S .

The only form for S which satisfies these conditions is given below, Where k is a positive constant.:

$$S = -k \sum P_i \ln P_i . \quad (1.8)$$

These information entropies can also be calculated over continuous probability distributions for model systems and real atoms, where the summation could be replaced by an integral,

$$S = -k \int P(x) \ln P(x) dx . \quad (1.9)$$

With an n dimensional $P(x_1, \dots, x_n)$ we have

$$S = -k \int \dots \int P(x_1, \dots, x_n) \ln P(x_1, \dots, x_n) dx \quad (1.10)$$

When one tries to measure conjugate observables, the uncertainty in one space has an inverse relation to uncertainty in the other space. This means that for a sharp distribution in position space, there will be a corresponding wide/diffuse distribution in momentum space and vice-versa. Jaynes [24] in his review article has related these uncertainties to information entropies in their respective spaces. A sharp distribution in any space will have a small information entropy value and a wide distribution will have a large information entropy value. The following curves show density distributions of a Gaussian and its Fourier transform, describing how a wide distribution in one space leads to sharp distribution in another space and vice versa for the following equations [25].

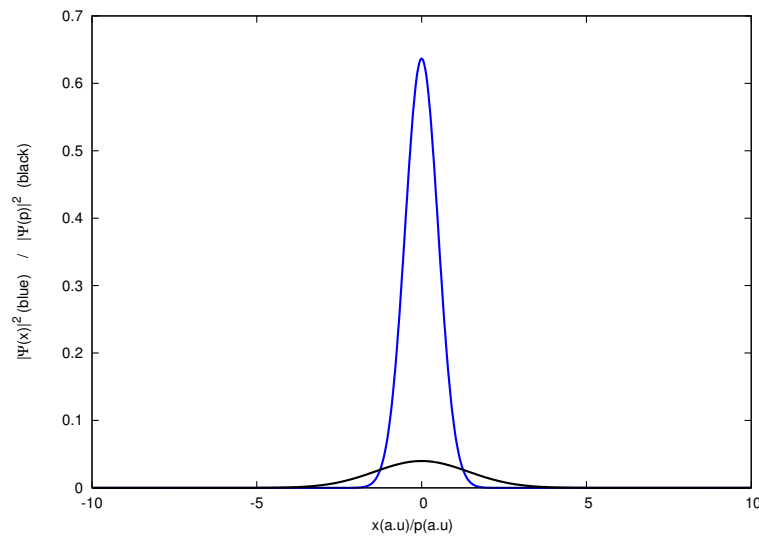


FIGURE 1.1: (a) *blue* : $|\Psi(x)|^2$
(b) *black* : $|\Psi(p)|^2$

$$\Psi(x) = \sqrt{\frac{\alpha}{\pi}} e^{-\alpha x^2} \quad @ \quad \alpha = 2.0 \quad \Psi(p) = \frac{1}{\sqrt{4\pi\alpha}} e^{-\frac{p^2}{4\alpha}} \quad @ \quad \alpha = 2.0$$

From now onwards we will use S_ρ and S_γ to denote information entropies in position space and momentum space respectively. In terms of the single particle charge density $\rho(\vec{r})$ and $\gamma(\vec{p})$

$$S_\rho = - \int \rho(\vec{r}) \ln \rho(\vec{r}) d^3r \quad S_\gamma = - \int \gamma(\vec{p}) \ln \gamma(\vec{p}) d^3p \quad (1.11)$$

1.5 Generalized uncertainty relations

Heisenberg uncertainty principle, in terms of variances in position and momentum, is denoted by $\Delta x \cdot \Delta p_x \geq \hbar$. Later, Kennard and Weyl calculated deviations in various model problems [26] and came up with a relation $\sigma_x \cdot \sigma_p \geq \frac{\hbar}{2}$, σ_x and σ_p are standard deviations in x and p spaces respectively.

The uncertainty in terms of information entropies is an extra bound on the physical system apart from the fundamental Heisenberg uncertainty principle [27]. This uncertainty relation says that $S_\rho + S_\gamma \geq n(1 + \ln \pi)$. One interesting result known is that, in the ground state, $S_\rho + S_\gamma$ is exactly equal to $1 + \ln \pi$ for the harmonic oscillator model problem. This is because there is a single gaussian representation of the ground state wave function in position and momentum space.

As given by Białyński-Birula and Mycielski, the $(p, q)^{\hbar}$ norm of the Fourier transform is given by the smallest number $k(p, q)$ for which the following inequality holds for all $\psi \in L^p$

$$\|\tilde{\psi}\|_q \leq k(p, q) \|\psi\|_p \quad (1.12)$$

where $\|\psi\|_p$ is given by,

$$\|\psi\|_p = \left(\int d^n r |\psi|^p \right)^{1/p} \quad (1.13)$$

and $k(p, q)$ is given by,

$$k(p, q) = \left(\frac{2\pi}{q} \right)^{n/2q} \left(\frac{2\pi}{p} \right)^{-n/2p} \quad (1.14)$$

Now re-writing eqn no 1.12 as,

$$W(q) = k(p, q) \|\psi\|_p - \|\tilde{\psi}\|_q \quad (1.15)$$

Where p and q are related by the following relation :

$$\frac{1}{p} + \frac{1}{q} = 1 \quad (1.16)$$

Now $W(q) \geq 0$. Parseval-Plancherel theorem says that this inequality becomes equality only for $q = 2$. Now expanding $W(q)$ and replacing p in terms of q .

$$W(q) = \left(\frac{2\pi}{q}\right)^{n/2q} \left(\frac{2\pi}{p}\right)^{-n/2p} \left[\int d^n r |\psi|^p \right]^{1/p} - \left[\int d^n k |\tilde{\psi}|^q \right]^{1/q} \quad (1.17)$$

From the previous relation $p = q/(q-1)$

$$W(q) = \left(\frac{2\pi}{q}\right)^{n/2q} \left(\frac{2\pi(q-1)}{q}\right)^{-nq/2(q-1)} \left[\int d^n r |\psi|^{(q-1)/q} \right]^{q/(q-1)} - \left[\int d^n k |\tilde{\psi}|^q \right]^{1/q} \quad (1.18)$$

Right derivative of $W(q)$ at $q=2$ should be non-negative.

$$\begin{aligned} & \frac{n}{4} N(1 + \ln \pi) - \frac{1}{2N} \int d^n r |\psi(r)|^2 \ln |\psi(r)|^2 \\ & - \frac{1}{2N} \int d^n k |\tilde{\psi}(k)|^2 \ln |\tilde{\psi}(k)|^2 + N \ln N \geq 0 \end{aligned} \quad (1.19)$$

Here $N = \|\psi\| = \|\tilde{\psi}\|$. For $N = 1$, the equation reduces to

$$-\langle \ln \rho \rangle - \langle \ln \tilde{\rho} \rangle \geq n(1 + \ln \pi) \quad (1.20)$$

Where $\rho(r) = |\psi(r)|^2$, $\tilde{\rho}(k) = |\tilde{\psi}(k)|^2$ and $\langle \ln \rho \rangle = \int d^n r \rho(r) \ln \rho(r)$

For real atoms the information entropy sum is expected to be greater than the equality i.e. $S_\rho + S_\gamma > n(1 + \ln \pi)$ and is expected to come close to the equality $n(1 + \ln \pi)$ in presence of external AC field with suitable field parameters (intensity and frequency). For the harmonic oscillator case we can change the system in such a way such that $S_\rho + S_\gamma$ for the ground state is exactly equal to $1 + \ln \pi$. However in field free conditions, it tends to increase rapidly with first few quantum states and then increase very slowly with higher quantum states. In the next section some aspects of the high frequency AC field will be discussed. On further reduction, the above bound reduces to the following equation. Gadre [28] has verified this new relation within Thomas-Fermi framework.

$$S_\rho + S_\gamma \geq 3N(1 + \ln \pi) - 2N \ln N \quad (1.21)$$

1.6 High Frequency AC fields

When any system is in the presence of a very high frequency AC field, at some particular field parameters (intensity and frequency), instead of destabilization there is a stabilization of the system. The AC field changes the potential so rapidly, such that the particle/system will remain localized inside the well. A decrease in information entropy sum is expected in these type of conditions due to confinement of bound states inside the well space. Since the bound states are said to be infinite lifetime states, their information will not change with time. There are other interesting effects such as, presence of a nearly-degenerate ground state, symmetry breaking in the wave function etc. The idea is to study the behaviour of entropies under high frequency AC field and field free conditions. One can achieve a system which is minimum in uncertainty by varying the field parameters (intensity and frequency). Also note that the uncertainty in terms of information entropies is dependent only on probability densities, which are experimentally measurable quantities.

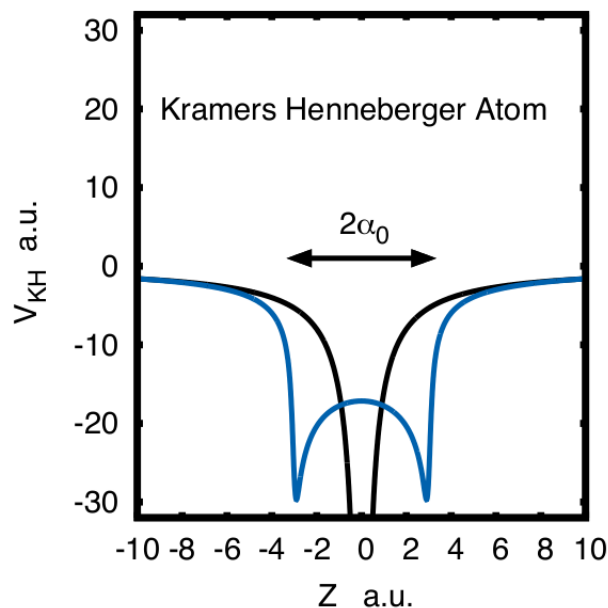


FIGURE 1.2: (a) $V(x)$ (in black) (b) V_0_{KH} (in blue)(effective non-ionizing potential for an atom)

From the Fig 1.2 one can easily interpret 1-D representation of a Coulombic potential which is infinity at the nuclear position becomes finite in presence of AC field. Also the attraction to the electrons comes from two “virtual” nuclei. The electrons which are in effect of coulombic potential are now in effect of zeroth order

Kramer-Henneberger potential [29] (and references therein). In the next section we will discuss Kramer-Henneberger transformation in detail.

1.7 Kramer-Henneberger transformation

Kramer-Henneberger transformation provides a theoretical framework for description of the system under high frequency AC fields [29] (and references therein). When system is exposed to any AC field, the potential part of the Hamiltonian become time dependent due to that AC field. For the Hamiltonian in Coulomb gauge, TDSE can be written as (a.u)

$$i\frac{\partial}{\partial t}\psi(x, t) = \left[-\frac{\nabla^2}{2} + v(x) + \epsilon x \cos \omega t \right] \psi(x, t) \quad (1.22)$$

$$U_1(x, t) = e^{-\frac{i\epsilon x}{\omega} \sin \omega t} \quad (1.23)$$

$$\chi(x, t) = U_1(x, t)\psi(x, t) \quad (1.24)$$

Applying a suitable unitary transformation and rewriting TDSE converts the Hamiltonian to a momentum gauge representation.

$$i\frac{\partial}{\partial t}\chi(x, t) = \left[-\frac{\nabla^2}{2} + v(x) + \frac{i\epsilon}{\omega} \sin(\omega t)\nabla + \frac{1}{2} \left(\frac{\epsilon}{\omega} \sin \omega t\right)^2 \right] \chi(x, t) \quad (1.25)$$

$$U_2(x, t) = e^{\frac{-\epsilon}{\omega^2} \cos(\omega t)\nabla} \quad (1.26)$$

$$\psi(x, t)' = U_1(x, t).U_2(x, t)\psi(x, t) \quad (1.27)$$

A series of such unitary transformations can take the Hamiltonian to the similar kind of system present in high frequency AC field conditions.

Similar operations can be applied to momentum space wave function by Fourier transforming position space wavefunction.

$$\psi(p, t) = \frac{1}{\sqrt{2\pi}} \int e^{-ipx} \psi(x, t) dx \quad (1.28)$$

Once the Hamiltonian and wave function of the system are defined, one can evaluate the energies and information entropies of the system for various states in dual spaces.

1.8 Motivation and plan of thesis

We have seen in earlier sections, the potential which is infinite due to presence of nucleus at the center becomes finite as if the nucleus is not even present there in the presence of high frequency, high intensity AC field and also in the same case two virtual nuclei come up in the picture equidistant from the center[29]. Under these conditions, there is stabilization. The chemistry under intense laser fields is entirely different. The information entropy sum in dual spaces are such that they tend to decrease in these intense laser fields resulting in minimized uncertainty and stabilization of the system. The idea is to figure out field parameters under which the system stabilizes itself by studying the information entropies of the various systems which are discussed in detail in the subsequent chapters.

Not many programs are available that calculate electron momentum densities on a grid, given a calculate electronic wavefunction in position space. The second chapter describes the details of a code written that calculates EMD.

In the third chapter, some of the model problems are discussed harmonic oscillator, Morse potential and Xenon potential. It is shown that they also have same kind of behaviour and try to minimize their entropy sum under intense laser fields. Also, an attempt is made to come up with a theoretical explanation for this kind of behaviour.

REFERENCES

- [1] Donald A. McQuarrie, John D. Simon, *Physical Chemistry: A Molecular Approach*
- [2] T. Kato, *Commun. Pure Appl. Math.* 10, 151 (1957).
- [3] E. J. Steiner, *J. Chem. Phys.* 39, 2365 (1963).
- [4] C. P. Yue and D. P. Chong, *Theoret. Chim. Acta (Berl.)* 12, 431 (1968).
- [5] J. A. Chapman and D. P. Chong, *Can. J. Chem.* 48, 2722 (1970).
- [6] M. M. Morrell, R. G. Parr and M. Levy, *J. Chem. Phys.* 62, 549 (1975).
- [7] M. Hoffmann-Ostenhof and T. Hoffmann-Ostenhof, *Phys. Rev. A* 16, 1782 (1977).
- [8] R. Ahlrichs, M. Hoffmann-Ostenhof, T. Hoffmann-Ostenhoff and J. D. Morgan III, *Phys. Rev. A* 23, 2106 (1981).
- [9] H. J. Silverstone, *Phys. Rev. A* 23, 1030 (1981).
- [10] H. Weinstein, P. Politzer and S. Srebrenik, *Theor. Chim. Acta (Berl.)* 38, 159 (1975).
- [11] A. M. Simas, R. P. Sagar, A. C. T. Ku and V. H. Smith Jr., *Can. J. Chem.* 66, 1923 (1988)
- [12] PhD thesis by P. Balanarayan “Three Dimensional Molecular Scalar Fields: A Topographical Perspective”.
- [13] B. Podolsky and L. Pauling, *Phys. Rev.* 34, 109 (1929).
- [14] P. Jordan, *Zeit. f. Phys.* 40, 809 (1927).
- [15] J. W. M. Du Mond, *Phys. Rev.* 33, 643 (1929).

-
- [16] W. C. Philips and R. J. Weiss, Phys. Rev. 171, 790 (1968).
- [17] C. A. Coulson, Proc. Camb. Phil. Soc. 37, 55 (1941).
- [18] C. A. Coulson, Proc. Camb. Phil. Soc. 37, 74 (1941).
- [19] C. A. Coulson, Mol. Phys. 26, 507 (1973).
- [20] P. Kaijser and V. H. Smith, Jr., in Quantum Science- Methods and Structure, Ed. J. L. Calais, O. Goscinski, J. Linderberg and Y. Ohrn, Plenum, New York, 1976.
- [21] A. J. Thakkar, J. Chem. Phys. 76, 746 (1982). T. Koga, H. Matsuyama, H. Inomata, E. Romera, J. S. Dehesa and A. J. Thakkar,
- [22] J. Chem. Phys. 109, 1601 (1998).
- [23] C. E. Shannon , *A Mathematical Theory of Communication*, The Bell System Technical Journal, Vol 27, p . 379-423,623-656 (1948)
- [24] E. T. Jaynes , *Information Theory and Statistical Mechanics*, The Physical Review, Vol 106, No. 4, p . 620-630 (1957)
- [25] Current Science, October 5, 1985, Vol. 54, No. 19.
- [26] Kennard, E. H. (1927), "Zur Quantenmechanik einfacher Bewegungstypen", Zeitschrift fr Physik (in German) 44 (45): 326, Bibcode:1927ZPhy...44..326K, doi:10.1007/BF01391200
- [27] Iwo Bialynicki-Birula, Jerzy Mycielski *Uncertainty Relations for Information Entropy in Wave Mechanics* , Commun, math. Phys, Vol 44, p . 129-132 (1975).
- [28] Gadre, S.R., Phys. Rev. A, 1984, 30, 620.
- [29] P. Balanarayan, Nimrod Moiseyev *Chemistry in high-frequency strong laser fields: the story of HeS molecule*, Molecular Physics, Vol 111, issue 12-13 p. 1814-1822 (2013).

Chapter 2

Program for Electron Density and Electron Momentum Density

2.1 Introduction

For calculating information entropies of atoms, single particle charge density is required at each point in 3-dimensional position and momentum spaces. These densities can not be analytically solved. These have to be numerically evaluated over a grid. The information entropies can not be analytically integrated as well. This is evident from the way electron densities are evaluated.

For an N -electron system, the position space single particle charge density is

$$\rho(\vec{r}) = N \sum_{\sigma} \int \Psi^*(\vec{r}, \vec{r}_2, \vec{r}_3, \dots, \vec{r}_N) \Psi(\vec{r}, \vec{r}_2, \vec{r}_3, \dots, \vec{r}_N) d^3 r_2 d^3 r_3 \dots d^3 r_N \quad (2.1)$$

The momentum space wavefunction is obtained by a Fourier transform of the position space wavefunction and is given by,

$$\Psi(\vec{p}_1, p_2, \vec{p}_3, \dots, \vec{p}_N) = \frac{1}{(2\pi)^{3N/2}} \int d^3 r_1 d^3 r_2 \dots d^3 r_N \Psi(\vec{r}_1, \vec{r}_2, \vec{r}_3, \dots, \vec{r}_N) e^{-i \sum_{i=1}^N \vec{r}_i \cdot \vec{p}_i} \quad (2.2)$$

For an N electrons system, the momentum space density is given by,

$$\gamma(\vec{p}) = N \sum_{\sigma} \int \Psi^*(\vec{p}, \vec{p}_2, \vec{p}_3, \dots, \vec{p}_N) \Psi(\vec{p}, \vec{p}_2, \vec{p}_3, \dots, \vec{p}_N) d^3 p_2 d^3 p_3 \dots d^3 p_N \quad (2.3)$$

Computationally, given molecular orbitals $\{\psi_a(\vec{r})\}$, the density is given by,

$$\rho(\vec{r}) = \sum_a |\psi_a(\vec{r})|^2 \quad (2.4)$$

It is to be remarked here, that to the best of our knowledge, there exist only 4 or 5 codes that evaluate momentum densities of atoms and molecules, given the molecular/atomic orbital coefficients of a Gaussian basis.

2.2 Electronic structure calculation

A molecular orbital is given by

$$\psi_a(\vec{r}) = \sum_{i=1}^N M_{(a,i)} C_i \phi_i \quad (2.5)$$

where N is the number of contractions present in the system. C_i is contraction level normalization and ϕ_i is i^{th} the contraction, which is a collection of primitive gaussians. $M_{(a,i)}$ are coefficients to a molecular orbital and are evaluated by running an electronic structure package GAMESS [1, 2] by providing ϕ_i in a certain format,

$$\phi_i = \sum_{k=1}^M a_k \chi_k \quad (2.6)$$

where i^{th} contraction contains M primitive gaussians and a_k is coefficient to a primitive gaussian and is required to be provided as GAMESS input. For position space,

$$\begin{aligned} \chi_k = (2\pi\alpha)^{3/4} & \left[\frac{(4\alpha)^{(l_k+m_k+n_k)/2}}{(2l_k-1)!! (2m_k-1)!! (2n_k-1)!!} \right]^{\frac{1}{2}} \\ & \times (x-x_a)^{l_k} (y-y_a)^{m_k} (z-z_a)^{n_k} e^{-\alpha_k[(x-x_a)^2+(y-y_a)^2+(z-z_a)^2]} \end{aligned} \quad (2.7)$$

For momentum space,

$$\begin{aligned} \chi_k = \frac{i^{l_k+m_k+n_k} l_k! m_k! n_k! \exp(-P^2/4\alpha + i\vec{P}\cdot\vec{A})}{(2\pi\alpha)^{3/4}} & \left[\frac{(4\alpha)^{(l_k+m_k+n_k)/2}}{(2l_k-1)!! (2m_k-1)!! (2n_k-1)!!} \right]^{1/2} \\ & \times \sum_{k_1=0}^{[l_k/2]} \frac{(-1)^{k_1} (p_x/\sqrt{\alpha})^{l_k-2k_1}}{k_1!(l_k-2k_1)!} \\ & \times \sum_{k_2=0}^{[m_k/2]} \frac{(-1)^{k_2} (p_y/\sqrt{\alpha})^{m_k-2k_2}}{k_2!(m_k-2k_2)!} \\ & \times \sum_{k_3=0}^{[n_k/2]} \frac{(-1)^{k_3} (p_z/\sqrt{\alpha})^{n_k-2k_3}}{k_3!(n_k-2k_3)!} \end{aligned} \quad (2.8)$$

where α_k is exponent for a particular primitive Gaussian. l_k, m_k, n_k are component of angular momentum in all three directions and x_a, y_a, z_a are position of atoms in three dimensional space. All these variables are required as GAMESS input. A sample input for the electronic structure calculation of Helium atom is given here.

```
$CONTRL SCFTYP=RHF RUNTYP=ENERGY $END
$DATA
HELIUM
C1
HE    2.0    0.0    0.0    0.0
      S    3
        1    502.89795759    0.0230741
        2    76.9896601    0.1681946
        3    17.98108986    0.8087312
      S    1
        1    0.18687559    1.0000000
      P    1
        1    9.4309800    1.0000000
      D    1
        1    7.2485900    1.0000000
      F    1
        1    1.522464995    1.0000000

$END
```

2.3 ED and EMD Code description

2.3.1 Primitives

The ED/EMD code developed here starts with accessing an input file *in.dat* which contains the following information:-

```
he1.dat
position/momentum
101
1001
```

- a. File Name:- This gives the information of file which needs to be extracted from that particular folder. Which contains coefficient to the wavefunctions and all basis information for a given atom.
- b. Density Type:- Information is passed on whether you are calculating position density or momentum density.
- c. Range:- This will give the range of the density type.
- d. No. of points:- This will give number of points in range while integration.

Now the code will read *he1.dat* which is a GAMESS input file for Helium EMD calculation. Inside the code one can find a function *initnocnpg* which accesses the file name and calculates number of contraction and number of primitive gaussians for the wave function from that file

In the next function *input* it stores the following parameters:-

- a. Atomic numbers of each element of the molecule.
- b. *MO coefficient's* in a two dimensional array.
- c. *K* and α values of the primitive gaussians.
- d. Number of primitive gaussians with respect to contractions.
- e. Angular momentum in all three directions with respect to contractions.
- f. Atom centres in all the three directions with respect to the atom

Following are three small functions which one can call anytime :-

- a.) *combination_function* for Combination function.
- b.) *factorial* for factorial function.
- c.) *dfact* for double factorial function.

2.3.2 Contraction level normalization

Inside the code one can find a function *cinorm* for calculating the contraction level normalization. For i^{th} contraction that contains M primitive gaussians:-

$$\phi_i = \sum_{k=1}^M a_k N_k \chi_k \quad (2.9)$$

$$N_k = \left(\frac{\alpha}{\pi}\right)^{3/4} \left[\frac{(4\alpha)^{(l_k+m_k+n_k)/2}}{(2l_k-1)!! (2m_k-1)!! (2n_k-1)!!} \right]^{1/2} \quad (2.10)$$

The contraction level normalization is given

$$C_i = \left[\frac{1}{\langle \phi_i | \phi_i \rangle} \right]^{\frac{1}{2}} \quad (2.11)$$

within a contraction the χ_k 's are not orthonormal and $\langle \phi_i | \phi_i \rangle$ is given by

$$\langle \phi_i | \phi_i \rangle = \sum_{s=1}^M \sum_{t=1}^M \langle a_s \chi_s | a_t \chi_t \rangle \quad (2.12)$$

where $\langle \chi_s | \chi_t \rangle$ is overlap integral and is given by

$$\begin{aligned} \langle \chi(\mathbf{A}, \alpha_1, l_1, l_2) | \chi(\mathbf{B}, \alpha_2, l_1, l_2) \rangle &= \pi^{3/2} \sigma^{3/2} \exp(-\alpha_1 \alpha_2 \sigma \overline{AB}) \\ &\times \sum_{i=0}^{(l_1+l_2)/2} f_{2i}(l_1, l_2, \overline{AB}_x, \overline{BP}_x) (2i-1)!! \left(\frac{\sigma}{2}\right)^i \\ &\times \sum_{j=0}^{(m_1+m_2)/2} f_{2j}(m_1, m_2, \overline{AB}_y, \overline{BP}_y) (2j-1)!! \left(\frac{\sigma}{2}\right)^j \\ &\times \sum_{k=0}^{(n_1+n_2)/2} f_{2k}(n_1, n_2, \overline{AB}_z, \overline{BP}_z) (2k-1)!! \left(\frac{\sigma}{2}\right)^k \end{aligned} \quad (2.13)$$

where $\sigma = 1/(\alpha_1 + \alpha_2)$. The expression for f_i 's is given by

$$(x+a)^{l_1} (x+b)^{l_2} = \sum_{i=0}^{l_1+l_2} f_i(l_1, l_2, a, b) x^i \quad (2.14)$$

Now, overall wave function of filled orbitals is given by :

$$\Psi_i = M_{(i,1)} C_1 \phi_1 + M_{(i,2)} C_2 \phi_2 + M_{(i,3)} C_3 \phi_3 + \dots \dots M_{(i,n)} C_n \phi_n$$

where Ψ_i is given by i^{th} filled orbital. The density evaluation on a grid is done using Eqn. 2.4. There is an analogous equation in momentum space.

The following process not only extracts this information but also generates report on separate report file *report.txt* in the same folder. Now, if one has the overall wave function which consist of all the filled orbitals of the system whether it is an atom or a molecule is known, we can extract the following properties of the system. [3]

From all the properties, three properties are very important in this whole scenario, namely:-

- a. Probability Density(both in position and momentum space)
- b. Information Entropy(both in position and momentum space)
- c. Kinetic Energy of the system.(for checking the correctness of the code)

| Atom | N_ρ | S_ρ | N_γ | S_γ | $S_\rho + S_\gamma$ |
|--------|----------|----------|------------|------------|---------------------|
| Helium | 1.99999 | 4.17416 | 1.99999 | 6.44125 | 10.61541 |

| Atom | K.E(Actual) | KE(Numerical) |
|--------|-------------|---------------|
| Helium | 2.86161 | 2.86152 |

| Atom | $S_\rho + S_\gamma$ | $\geq 3N(1 + \ln\pi) - 2N \ln N$ |
|------|---------------------|----------------------------------|
| He | 10.61541 | 10.0957 |

$S_\rho + S_\gamma$ are denoted as sum of information entropy in dual space and is expected to come out to higher than $S_\rho + S_\gamma \geq 3N(1 + \ln\pi) - 2N \ln N$. Where 3 is number of dimensions in position and momentum space and N is the number of particles in the system.

2.4 Results

The fig 2.1 is the probability densities for Helium in position spaces at $Z = 0.0 \text{ a.u.}$
Fig 2.2 is the probability densities for Helium in position spaces at $Y = 0.0 \text{ a.u.}$
 $Z = 0.0 \text{ a.u.}$

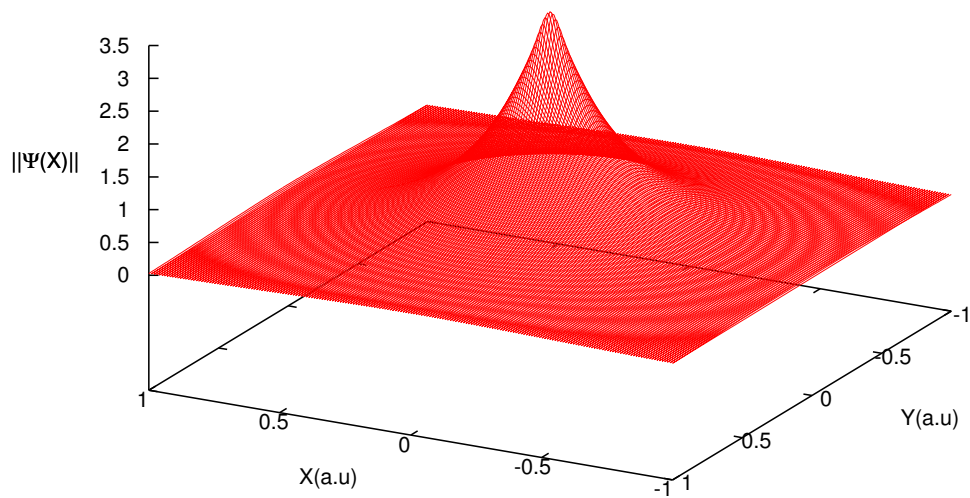


FIGURE 2.1: Helium in position space at $Z = 0 \text{ (a.u.)}$.

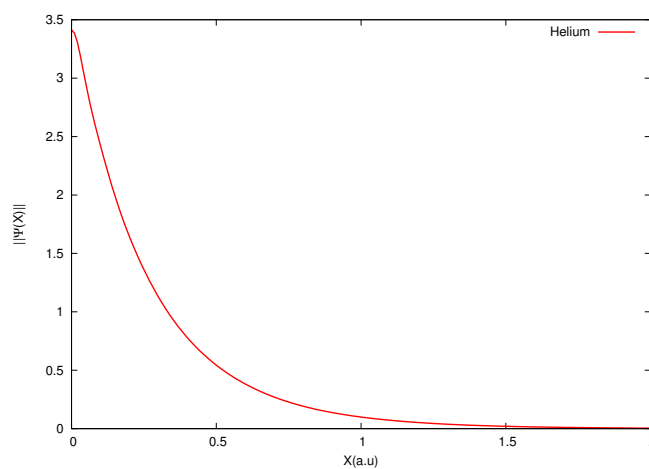


FIGURE 2.2: Helium in position space at $Y = Z = 0.0 \text{ (a.u.)}$.

The fig 2.3 is the probability densities for Helium in momentum spaces at $P_Z = 0.0 \text{ a.u.}$ Fig 2.4 is the probability densities for Helium in momentum spaces at $P_Y = 0.0 \text{ a.u.}$ and $P_Z = 0.0 \text{ a.u.}$

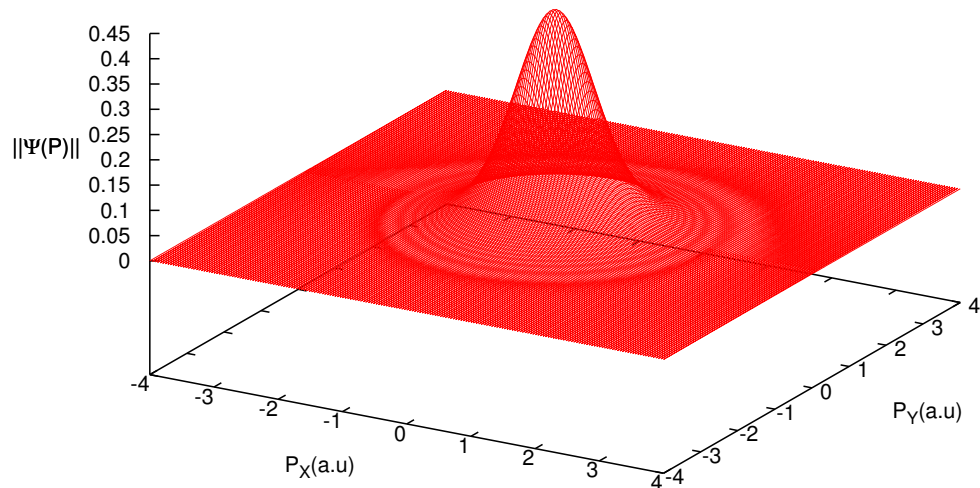


FIGURE 2.3: Helium in momentum space at $P_Z = 0 \text{ (a.u.)}$.

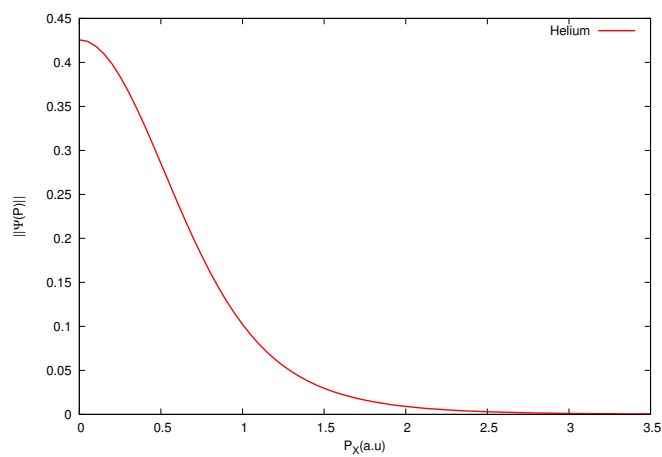


FIGURE 2.4: Helium in momentum space at $P_Y = P_Z = 0.0 \text{ (a.u.)}$.

REFERENCES

- [1] "General Atomic and Molecular Electronic Structure System" M.W.Schmidt, K.K.Baldrige, J.A.Boatz, S.T.Elbert, M.S.Gordon, J.H.Jensen, S.Koseki, N.Matsunaga, K.A.Nguyen, S.Su, T.L.Windus, M.Dupuis, J.A.Montgomery J. Comput. Chem., 14, 1347-1363(1993).
- [2] "Advances in electronic structure theory: GAMESS a decade later" M.S.Gordon, M.W.Schmidt pp. 1167-1189, in "Theory and Applications of Computational Chemistry: the first forty years" C.E.Dykstra, G.Frenking, K.S.Kim, G.E.Scuseria (editors), Elsevier, Amsterdam, 2005.
- [3] Attila Szabo, Neil S. Ostlund, Modern Quantum Chemistry: Introduction to Advanced Electronic Structure Theory.

Chapter 3

Model Problems

The understanding of a bigger picture is incomplete without simple examples or model problems. In this chapter, the information entropies of some model quantum systems have been numerically evaluated as a function of AC field parameters. The first one is the purely harmonic oscillator in which all the states are bound by the potential. The second one is the Morse potential which is an approximation to real vibrational systems with a limited number of bound states. The $S_\rho + S_\gamma$ for the ground state is very near to $1 + \ln \pi$ and continues to remain constant as we increase α_0 which is field parameter for laser intensity and frequency. The third one is Xenon model potential in which two states are perfectly bound and one state which is bound but very near to the continuum. For this case, it has been found that $S_\rho + S_\gamma$ goes through a minimum and then increases as α_0 is increased .

3.1 Harmonic Oscillator

The information entropies found for this kind of system are similar to that of uncertainty principle given by Heisenberg. A precise measurement in one space will consequently result in a very large uncertainty in other space. A broad distribution leads to a higher information entropic value than a sharp distribution. The following equations represent normalized wavefunctions of the simple harmonic oscillator in position space

$$\Psi_v(x) = \left(\frac{\sigma}{\pi}\right)^{1/4} \frac{1}{\sqrt{2^v v!}} H_v(\sqrt{\sigma}x) e^{-\frac{\sigma}{2}x^2} \quad (3.1)$$

The corresponding momentum space representation is given by

$$\Psi_v(p) = i^v \left(\frac{1}{\sigma\pi}\right)^{1/4} \frac{1}{\sqrt{2^v v!}} H_v\left(\frac{1}{\sqrt{\sigma}}p\right) e^{-\frac{1}{2\sigma}p^2} \quad (3.2)$$

3.1.1 Case 1 : $\sigma > 1$

In this case there is a sharp distribution in position space and a wide distribution in momentum space. Consequently there will be lower information entropy in position space than in the momentum space w.r.t quantum state. In the Fig 3.1, the blue lines represent the probability densities in position space $|\psi(x)|^2$ and the black lines represent the probability densities in momentum space $|\psi(p)|^2$. The potential is plotted in red.

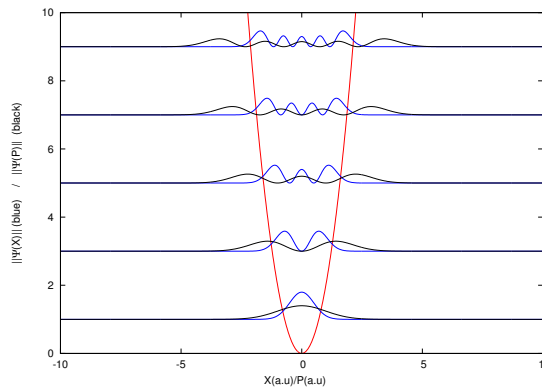


FIGURE 3.1: Probability densities in position and momentum space for $\sigma > 1$.

The information entropies in their respective space and total information entropy sum are plotted w.r.t vibrational state. In the Fig 3.2, the blue lines represent information entropies in position space S_ρ and the black line represents the information entropies in momentum space S_γ . The red line represent the total information entropy sum in dual spaces, $S_\rho + S_\gamma$.

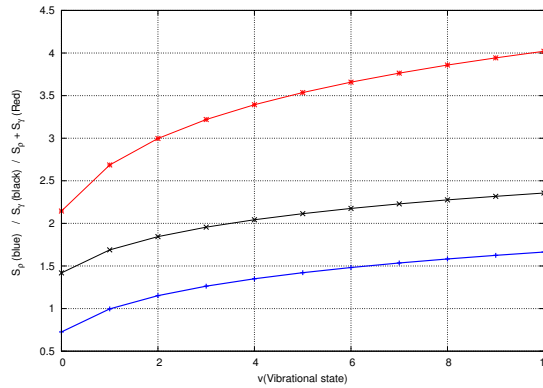


FIGURE 3.2: Information entropies in position and momentum space as a function of vibrational state for $\sigma > 1$.

3.1.2 Case 2 : $\sigma < 1$

In this case, there is a wide distribution in position space and a sharp distribution in momentum space. Consequently there will be higher Information entropy in position space than in the momentum space w.r.t quantum state. In the Fig 3.3, the blue line represent the probability densities in position and the black line represent the probability densities in momentum space. The potential is plotted in red.

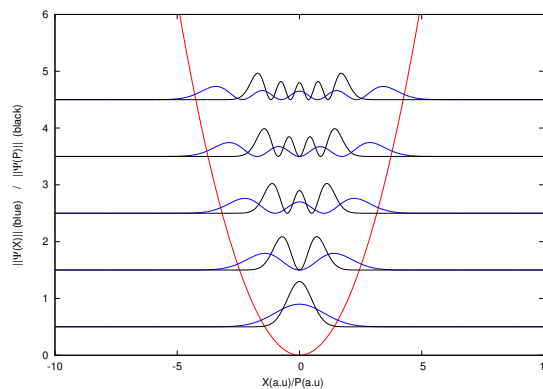


FIGURE 3.3: Probability densities in position and momentum space for $\sigma < 1$.

The information entropies in their respective space and total information entropy sum is plotted w.r.t vibrational state. In the Fig 3.4, the blue lines represent information entropies in position space S_p and the black line represent the information entropies in momentum space S_γ . The red line is the total information entropy sum in dual spaces $S_p + S_\gamma$.

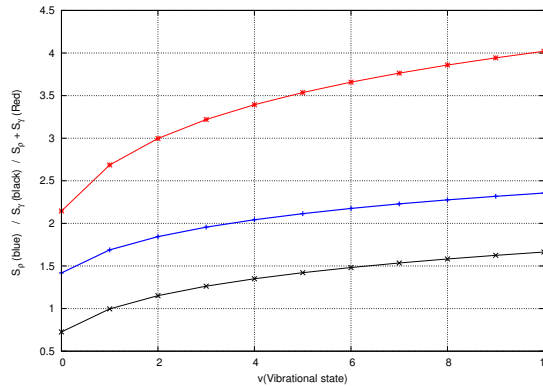


FIGURE 3.4: Information entropies in position and momentum space as a function of vibrational state for $\sigma < 1$.

3.1.3 Case 3 : $\sigma = 1$

In this case we have equal distribution in position and momentum space. Consequently the values for information entropy in position and momentum will be equal space w.r.t quantum state. In the Fig 3.5 the green line represents the probability densities in position and the black lines represents the probability densities in momentum space. The potential is plotted in red. Since there is an equal distribution in position and momentum space the probability density plot exactly overlap each other.

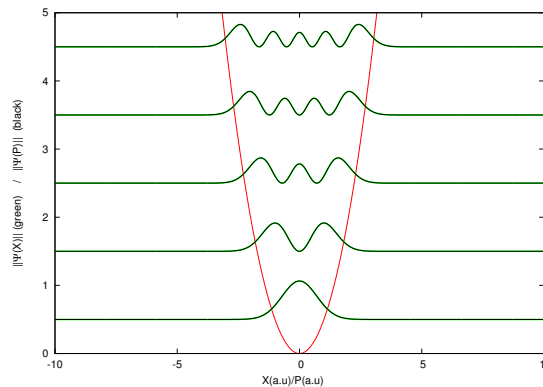


FIGURE 3.5: Probability densities in position and momentum space for $\sigma = 1$.

The information entropies in their respective space and total information entropy sum is plotted w.r.t vibrational state. In the Fig 3.6, the blue line represent information entropies in position space S_ρ and the black line represents the information entropies in momentum space S_γ . The red line is the total information entropy sum in dual spaces, $S_\rho + S_\gamma$.

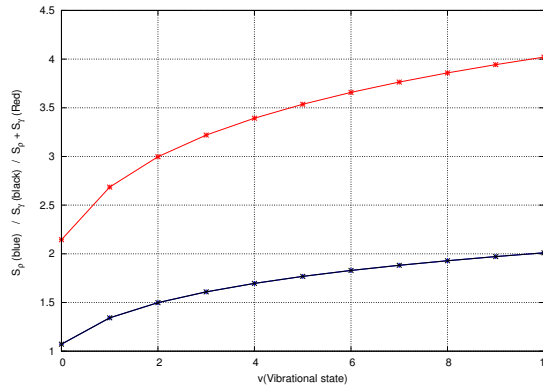


FIGURE 3.6: Information entropies in position and momentum space as a function of vibrational state for $\sigma = 1$ in which there is an equal distribution in position and momentum space.

In all the above three cases, it is important to note that S_ρ and S_γ vary for the change in σ but $S_\rho + S_\gamma$ is invariant of σ .

3.1.4 KH Transformation on a harmonic oscillator potential

In this section, a theoretical framework for harmonic oscillator system under high frequency AC field is explained. The TDSE for harmonic oscillator under AC field is given by

$$i \frac{\partial}{\partial t} \psi(x, t) = \left[-\frac{\nabla^2}{2} + V(x) + \epsilon x \cos \omega t \right] \psi(x, t) \quad (3.3)$$

The last term in this Hamiltonian expression is the interaction of the system with the AC field. Also, the effective Hamiltonian include dipole interaction in presence of AC field. Where $V(x) = \frac{1}{2}kx^2$ and ϵ is the field intensity parameter. Applying a suitable unitary transformation:

$$U(x, t) = e^{-\frac{i\epsilon x}{\omega} \sin \omega t} \quad (3.4)$$

$$i \frac{\partial}{\partial t} \psi(x, t) = \left[-\frac{\nabla^2}{2} + V(x) + \frac{i\epsilon}{\omega} \sin(\omega t) \nabla + \frac{1}{2} \left(\frac{\epsilon}{\omega} \sin \omega t \right)^2 \right] \psi(x, t) \quad (3.5)$$

where ω is the frequency of the AC field. A further applying of suitable unitary transformation will take the Hamiltonian to,

$$U(x, t) = e^{\frac{-\epsilon}{\omega^2} \cos(\omega t) \nabla} \quad (3.6)$$

$$i \frac{\partial}{\partial t} \psi(x, t) = \left[-\frac{\nabla^2}{2} + \frac{\epsilon^2}{2\omega^2} \sin^2 \omega t + V(x + \frac{\epsilon}{\omega^2} \cos \omega t) \right] \psi(x, t) \quad (3.7)$$

Now, $\alpha_0 = \frac{\epsilon}{\omega^2}$, which is a commonly used laser parameter comprising of both i.e. intensity and frequency. Expanding out $V(x + \alpha_0 \cos \omega t)$ we get,

$$i \frac{\partial}{\partial t} \psi(x, t) = \left[-\frac{\nabla^2}{2} + \frac{\epsilon^2}{2\omega^2} \sin^2(\omega t) + \frac{kx^2}{2} + \frac{k\alpha_0^2}{2} \cos^2 \omega t + kx\alpha_0 \cos \omega t \right] \psi(x, t) \quad (3.8)$$

Applying first set of unitary transformations.

$$U(x, t) = e^{\frac{-ikx\alpha_0}{\omega} \sin \omega t} \quad (3.9)$$

$$i \frac{\partial}{\partial t} \psi(x, t) = \left[\frac{\epsilon^2}{2\omega^2} \sin^2(\omega t) + \frac{kx^2}{2} + \frac{k\alpha_0^2}{2} \cos^2 \omega t - \frac{\nabla^2}{2} + \frac{ik\alpha_0}{\omega} \sin \omega t \nabla + \frac{1}{2} \left(\frac{k\alpha_0}{\omega} \sin \omega t \right)^2 \right] \psi(x, t) \quad (3.10)$$

$$U(x, t) = e^{\frac{-k\alpha_0}{\omega^2} \cos \omega t \nabla} \quad (3.11)$$

$$i \frac{\partial}{\partial t} \psi(x, t) = \left[\frac{\epsilon^2}{2\omega^2} \sin^2(\omega t) + \frac{k\alpha_0^2}{2} \cos^2 \omega t - \frac{\nabla^2}{2} + \frac{1}{2} \left(\frac{k\alpha_0}{\omega} \sin \omega t \right)^2 + \frac{kx^2}{2} + \frac{k^2 \alpha_0 x}{\omega^2} \cos \omega t + \frac{k}{2} \left(\frac{k\alpha_0}{\omega^2} \cos \omega t \right)^2 \right] \psi(x, t) \quad (3.12)$$

The last three terms in equation (3.12) will be again of the form : $\frac{k}{2} \left(x + \frac{k\alpha}{\omega^2} \cos \omega t \right)^2$.

Applying second set of unitary transformations,

$$U(x, t) = e^{\frac{-ik^2 x \alpha_0}{\omega^3} \sin \omega t} \quad (3.13)$$

$$i\frac{\partial}{\partial t}\psi(x,t) = \left[\frac{\epsilon^2}{2\omega^2}\sin^2(\omega t) + \frac{k\alpha_0^2}{2}\cos^2 \omega t + \frac{1}{2}\left(\frac{k\alpha_0}{\omega}\sin \omega t\right)^2 + \frac{kx^2}{2} + \frac{k}{2}\left(\frac{k\alpha_0}{\omega^2}\cos \omega t\right)^2 - \frac{\nabla^2}{2} + \frac{ik^2\alpha_0}{\omega^2}\sin \omega t\nabla + \frac{1}{2}\left(\frac{k^2\alpha_0}{\omega^3}\sin^2\omega t\right) \right]\psi(x,t) \quad (3.14)$$

$$U(x,t) = e^{\frac{-k^2\alpha_0}{\omega^4}\cos \omega t\nabla} \quad (3.15)$$

$$i\frac{\partial}{\partial t}\psi(x,t) = \left[\frac{\epsilon^2}{2\omega^2}\sin^2(\omega t) + \frac{k\alpha_0^2}{2}\cos^2 \omega t + \frac{1}{2}\left(\frac{k\alpha_0}{\omega}\sin \omega t\right)^2 - \frac{k}{2}\left(\frac{k\alpha_0}{\omega^2}\cos \omega t\right)^2 - \frac{\nabla^2}{2} + \frac{1}{2}\left(\frac{k^2\alpha_0}{\omega^3}\sin^2\omega t\right) + \frac{kx^2}{2} + \frac{k^3x\alpha_0\cos \omega t}{\omega^4} + \frac{k}{2}\left(\frac{k^2\alpha_0\cos \omega t}{\omega^4}\right)^2 \right]\psi(x,t) \quad (3.16)$$

The n^{th} set of unitary transform will lead to TISE under high frequency AC field conditions,

$$i\frac{\partial}{\partial t}\psi(x,t) = \left[\frac{\epsilon^2}{2\omega^2}\sin^2(\omega t) - \frac{\nabla^2}{2} + \frac{k}{2}(\alpha_0\cos \omega t)^2 + \frac{kx^2}{2} + \frac{1}{2}\sum_{i=1,j=1}^{i=n,j=2n} \left\{ \frac{k^i\alpha_0\sin \omega t}{\omega^j} \right\}^2 + \frac{k}{2}\sum_{i=1,j=2i-2}^{i=n,j=2n} C_1 \left\{ \frac{k^{i-1}\alpha_0\cos \omega t}{\omega^j} \right\}^2 + \frac{ik^n\alpha_0\sin \omega t}{\omega^{2(n-1)+1}}\nabla \right]\psi(x,t) \quad (3.17)$$

Where, in the equation (3.17) $C_1 = 0; i = 1$ and $C_1 = 1; i > 1$.

$$i\frac{\partial}{\partial t}\psi(x,t) = \left[\frac{\epsilon^2}{2\omega^2}\sin^2(\omega t) - \frac{\nabla^2}{2} + \frac{k}{2}(\alpha_0\cos \omega t)^2 + \frac{kx^2}{2} + \frac{1}{2}\sum_{i=1,j=1}^{i=n,j=2n} \left\{ \frac{k^i\alpha_0\sin \omega t}{\omega^j} \right\}^2 + \frac{k}{2}\sum_{i=1,j=2i}^{i=n,j=2n} \left\{ \frac{k^i\alpha_0\cos \omega t}{\omega^j} \right\}^2 + \frac{k^{n+1}\alpha_0x\cos \omega t}{\omega^{2n}} \right]\psi(x,t) \quad (3.18)$$

Under high frequency conditions the time dependence vanishes from the problem. Now if the direction of the AC field is reversed. The TDSE will be given by :

$$i\frac{\partial}{\partial t}\psi(x,t) = \left[-\frac{\nabla^2}{2} + v(x) - \epsilon x \cos \omega t \right]\psi(x,t) \quad (3.19)$$

The initial Coulomb and momentum gauge unitary transformation will lead to:

$$i \frac{\partial}{\partial t} \psi(x, t) = \left[-\frac{\nabla^2}{2} - \frac{\epsilon^2}{2\omega^2} \sin^2 \omega t + v\left(x - \frac{\epsilon}{\omega^2} \cos \omega t\right) \right] \psi(x, t) \quad (3.20)$$

Expanding out $v\left(x - \frac{\epsilon}{\omega^2} \cos \omega t\right)$ we get,

$$i \frac{\partial}{\partial t} \psi(x, t) = \left[-\frac{\nabla^2}{2} - \frac{\epsilon^2}{2\omega^2} \sin^2(\omega t) + \frac{kx^2}{2} + \frac{k\alpha^2}{2} \cos^2 \omega t - \right. \\ \left. kx\alpha \cos \omega t \right] \psi(x, t) \quad (3.21)$$

For this TDSE, the n^{th} set of Coulomb and momentum gauge unitary transformations will lead to TISE under high frequency AC field conditions:

$$i \frac{\partial}{\partial t} \psi(x, t) = \left[\frac{-\epsilon^2}{2\omega^2} \sin^2(\omega t) - \frac{\nabla^2}{2} + \frac{k}{2} (\alpha \cos \omega t)^2 + \frac{kx^2}{2} - \frac{1}{2} \sum_{i=1, j=1}^{i=n, j=2n} \left\{ \frac{k^i \alpha \sin \omega t}{\omega^j} \right\}^2 + \right. \\ \left. \frac{k}{2} \sum_{i=1, j=2i-2}^{i=n, j=2n} C_1 \left\{ \frac{k^{i-1} \alpha \cos \omega t}{\omega^j} \right\}^2 - \frac{ik^n \alpha \sin \omega t}{\omega^{2(n-1)+1}} \nabla \right] \psi(x, t) \quad (3.22)$$

Where, in the equation (3.22) $C_1 = 0; i = 1$ and $C_1 = 1; i > 1$.

$$i \frac{\partial}{\partial t} \psi(x, t) = \left[\frac{-\epsilon^2}{2\omega^2} \sin^2(\omega t) - \frac{\nabla^2}{2} + \frac{k}{2} (\alpha \cos \omega t)^2 + \frac{kx^2}{2} - \frac{1}{2} \sum_{i=1, j=1}^{i=n, j=2n} \left\{ \frac{k^i \alpha \sin \omega t}{\omega^j} \right\}^2 + \right. \\ \left. \frac{k}{2} \sum_{i=1, j=2i}^{i=n, j=2n} \left\{ \frac{k^i \alpha \cos \omega t}{\omega^j} \right\}^2 - \frac{k^{n+1} \alpha x \cos \omega t}{\omega^{2n}} \right] \psi(x, t) \quad (3.23)$$

Under high frequency conditions the time dependence vanishes from the problem.

3.1.5 Minimum Information Entropy Driving

The Hamiltonian for harmonic oscillator in field free conditions is given by

$$H = \left[-\frac{\nabla^2}{2} + V(x) \right] \quad (3.24)$$

$$V(x) = \frac{1}{2}kx^2 \quad (3.25)$$

The Hamiltonian for harmonic oscillator under intense AC field is given by

$$H_{KH} \left[-\frac{\nabla^2}{2} + V_{KH} \right] \quad (3.26)$$

where V_{KH} is the new effective potential

$$V_{KH} = \frac{1}{2}kx^2 + C \quad (3.27)$$

where C is a constant by which potential is actually shifted up. The constant C depends upon the intensity and frequency of the AC field. The exact description is given in next section.

Now the potential V_{KH} can be shifted up in a way such that the ground state for the V_{KH} matches exactly with excited state of the previous $V(x)$. In this way we will have a state in which the information entropy is minimum and is equal to $1 + \ln \pi$. It should be noted that the energy of the new ground state is no longer same.

The potential V_{KH} can be shifted up in a way such that any state for the V_{KH} matches exactly with the any higher excited state of the previous $V(x)$. In this way we will have a state in which the Information entropy is minimum but will be higher $1 + \ln \pi$.

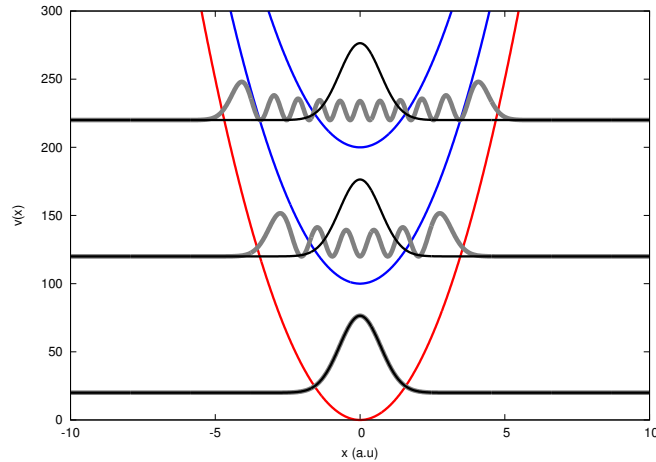


FIGURE 3.7: Ground state driving of V_{KH} (in blue) of harmonic Oscillator to 5^{th} and 10^{th} excited state of previous $V(x)$ (in Red) under Kh Transformation.

$S_\rho + S_\gamma$ is invariant with α . From the Figs 3.2, 3.4, 3.6 it can be seen that the value of $S_\rho + S_\gamma$ is exactly equal to $1 + \ln\pi$ for the ground state of the harmonic oscillator and continue to increase upto a certain point with vibrational state. Fig 3.7 is the depiction for how one can drive a system such that the ground state information is still exactly equal to $1 + \ln\pi$ but the ground state is no more the same. This happens because in the KH framework the effective Hamiltonian now differs by a constant, which is nothing but change in the potential energy of the system.

3.2 MORSE POTENTIAL

The tool used is generic DVR under fourier basis $\frac{1}{\sqrt{L}}e^{i2n\pi x/L}$ to solve the Schrödinger equation. The idea here is to construct the Hamiltonian matrix which comprises of kinetic and potential energy elements. The only non-zero, diagonal kinetic energy elements are simply given by, $\frac{4n^2\pi^2\hbar^2}{2mL^2}$.

$$\begin{aligned}
 \langle T \rangle &= \frac{-\hbar^2}{2m} \frac{1}{L} \int_0^L e^{-i2n\pi x/L} \frac{d^2}{dx^2} e^{i2n\pi x/L} dx \\
 &= \frac{-\hbar^2}{2m} \frac{1}{L} \left[\frac{i2n\pi}{L} \right]^2 L \\
 &= \frac{\hbar^2}{2m} \frac{1}{L} \left[\frac{2n\pi}{L} \right]^2 L
 \end{aligned} \tag{3.28}$$

For setting up the potential energy matrix in this basis, the expectation value $\langle \hat{x} \rangle_{jk}$ calculated as,

$$\begin{aligned}
 \langle \hat{x} \rangle_{jk} &= \frac{1}{L} \int_0^L e^{-i2\pi jx/L} x e^{i2\pi kx/L} dx \\
 &= \frac{1}{L} \int_0^L x e^{-i2\pi(j-k)x/L} dx \\
 &= \frac{iL}{2(j-k)\pi}
 \end{aligned} \tag{3.29}$$

The resultant matrix is diagonalized and finally the effective potential is evaluated at those grid points. Computationally AC field parameter shows up only in this potential energy matrix only and does not affect the kinetic energy part. This is evaluated using Gauss Legendre integration $V_0 = \frac{1}{2\pi} \int_0^{2\pi} V(x - \alpha_0 \cos \tau) d\tau$, where $V(x)$ can be any arbitrary potential which can be analytically defined.

The corresponding momentum basis function is obtained by Fourier transforming position space basis function.

$$\begin{aligned}
 \phi_n(p) &= \frac{1}{\sqrt{2\pi}} \int_0^L e^{-ipx} \phi_n(x) \\
 &= \frac{1}{\sqrt{2\pi}} \int_0^L e^{-ipx} \frac{1}{\sqrt{L}} e^{i2n\pi x/L} \\
 &= \frac{1}{\sqrt{2\pi L}} \frac{1}{((2n\pi/L) - p)} [e^{i((2n\pi/L)-p)L} - 1]
 \end{aligned} \tag{3.30}$$

The following equation is representation of typical one dimensional morse potential

$$V(x) = D_e(1 - e^{-\beta(x-x_e)})^2 \tag{3.31}$$

The information entropies were evaluated as a function of α_0 for H_2 molecule where the parameters for the morse potential are

$$D_e = 0.1745412844 \text{ a.u.}, \quad \beta = -1.0213174 \text{ a.u.}, \quad x_e = -1.400279678 \text{ a.u.}$$

Fig 3.8 depict the effective potential under α_0 . The ground state energy is increasing with α_0 . The higher states energy will also increase in a certain fashion and is depicted in the next section.

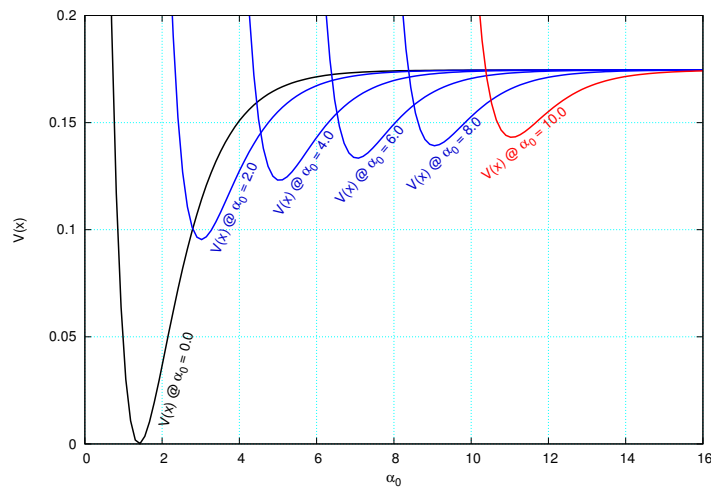


FIGURE 3.8: Morse potential for hydrogen molecule as a function of α_0 .

The Fig 3.9 shows energy levels in free field conditions i.e. at α_0 . The Fig 3.10 shows how first few state energies vary as we increase α_0 . There are 17 bound states in

field free conditions for the choices of parameter. The number of bound state are decreasing and the remaining bound states are squeezing inside the potential as α_0 , the AC field parameter is increasing. In the smaller plot, the energy less than 0.17451 a.u. is bound state. The last bound state is the gray one. In the same smaller plot, the last two states are not bounded by the potential.

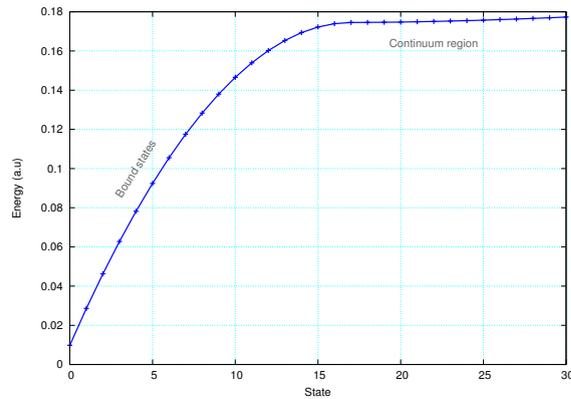


FIGURE 3.9: Energy levels for morse potential for hydrogen molecule.

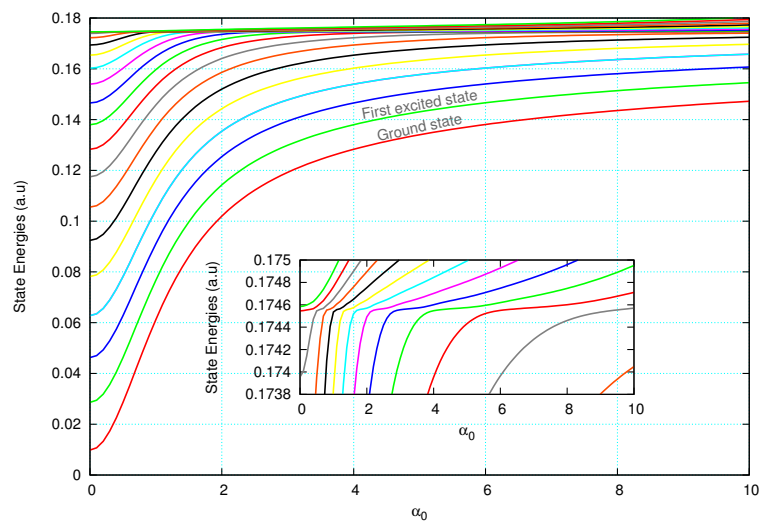


FIGURE 3.10: State Energies for morse potential for hydrogen molecule as a function of α_0 .

Fig show probability density plot in both spaces for the first two states w.r.t α_0 . In the next section, S_ρ is increasing with α_0 , which is here supported by broad distribution in position space with α_0 . S_γ was decreasing with α_0 , which is also supported here by sharp distribution in momentum space with α_0 .

Note : In the Fig 3.11 and 3.12 the probability desities are absolute and are not zero point corrected.

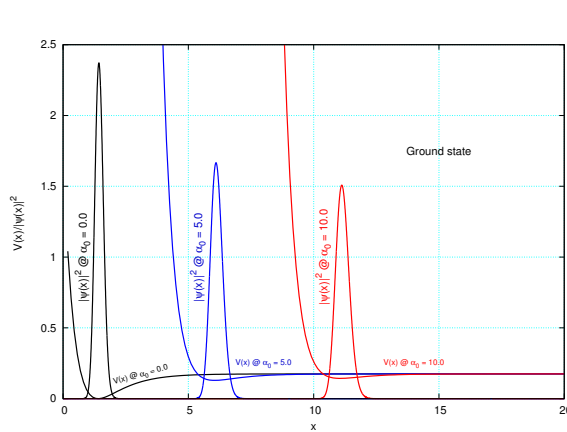


FIGURE 3.11: Morse potential for hydrogen molecule and Probabil-ity densities for Ground state in position space as function of α_0

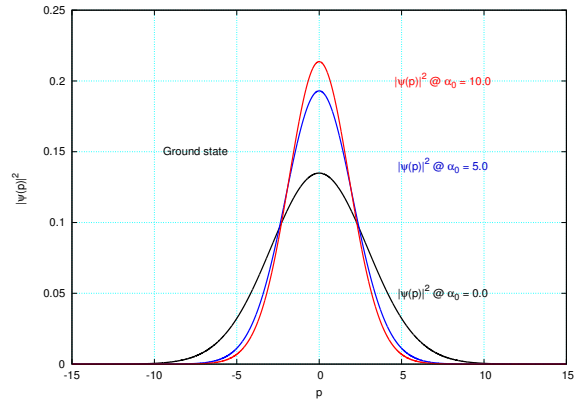


FIGURE 3.13: The corresponding Probability densities for Ground state in momentum space as func-tion of α_0

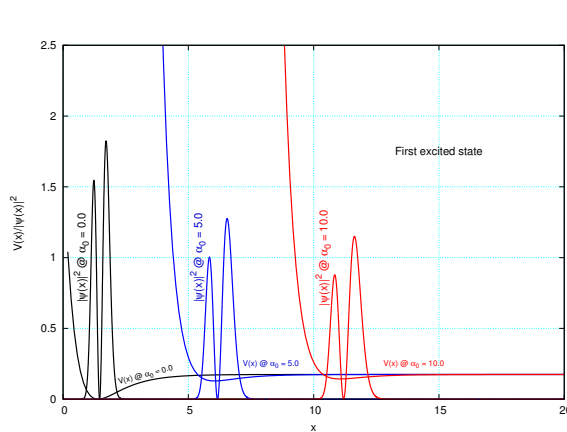


FIGURE 3.12: Morse potential for hydrogen molecule and Probabil-ity densities for First excited state in position space as function of α_0

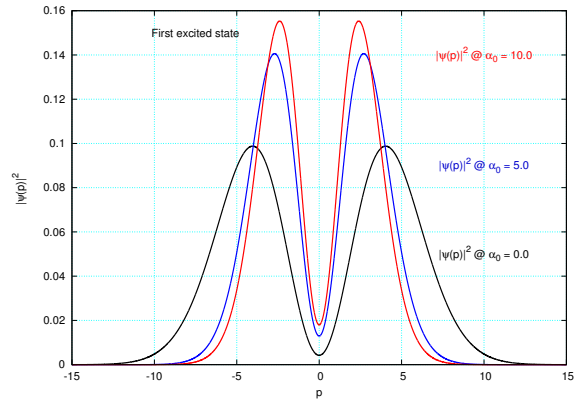


FIGURE 3.14: The corresponding Probability densities for First excited state in momentum space as function of α_0

The following curves show how S_ρ , S_γ and $S_\rho + S_\gamma$ for ground and the first excited state vary with α_0 . For both states, S_ρ is increasing with α_0 and S_γ is decreasing with α_0 . The smaller plot only shows how $S_\rho + S_\gamma$ vary with α_0 . From these smaller plots one can clearly see that $S_\rho + S_\gamma$ is increasing very slowly w.r.t α_0 .

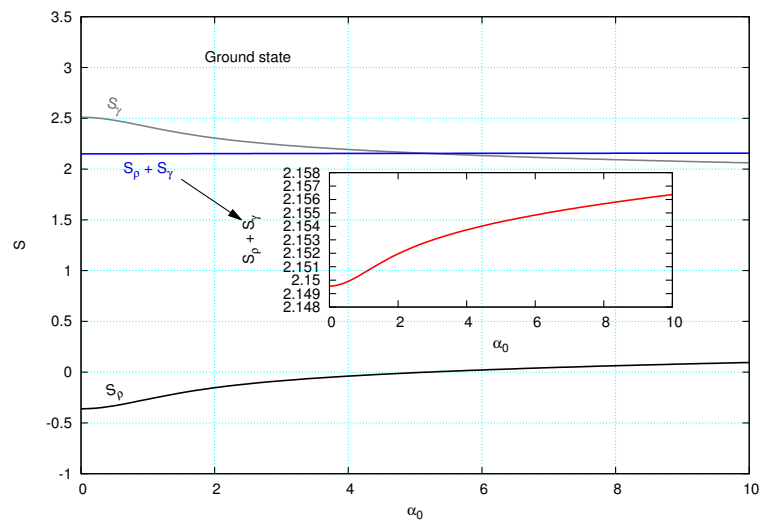


FIGURE 3.15: Ground state Information entropies as a function of α_0

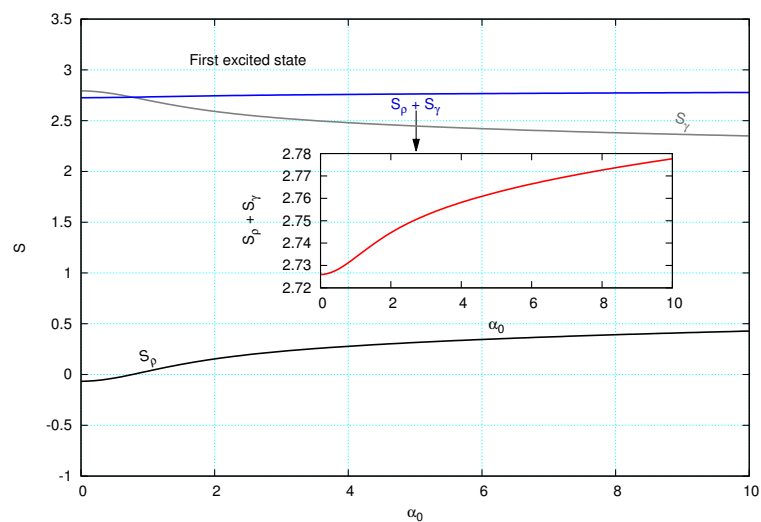


FIGURE 3.16: First excited state Information entropies as a function of α_0

3.3 XENON POTENTIAL

The same tool used is generic DVR under fourier basis $\frac{1}{\sqrt{L}}e^{i2n\pi x/L}$ to solve the Schrödinger equation. For setting up the Hamiltonian matrix which comprises of kinetic and potential energy elements. The only non-zero, diagonal kinetic energy elements are simply given by, $\frac{4n^2\pi^2\hbar^2}{2mL^2}$.

$$\begin{aligned}
 \langle T \rangle &= \frac{-\hbar^2}{2m} \frac{1}{L} \int_{-L/2}^{L/2} e^{-i2n\pi x/L} \frac{d^2}{dx^2} e^{i2n\pi x/L} dx \\
 &= \frac{-\hbar^2}{2m} \frac{1}{L} \left[\frac{i2n\pi}{L} \right]^2 L \\
 &= \frac{\hbar^2}{2m} \frac{1}{L} \left[\frac{2n\pi}{L} \right]^2 L
 \end{aligned} \tag{3.32}$$

The potential energy matrix in this basis is evaluated by obtaining the expectation value $\langle \hat{x} \rangle_{jk}$.

$$\begin{aligned}
 \langle \hat{x} \rangle_{jk} &= \frac{1}{L} \int_{-L/2}^{L/2} e^{-i2\pi jx/L} x e^{i2\pi kx/L} dx \\
 &= \frac{1}{L} \int_{-L/2}^{L/2} x e^{-i2\pi(j-k)x/L} dx \\
 &= \frac{iL}{2(j-k)\pi} (-1)^{-(j-k)}
 \end{aligned} \tag{3.33}$$

The resultant matrix is diagonalized and then finally the effective potential is evaluated at those grid points. Computationally the role of AC field parameter is only in this potential energy matrix and is evaluated using Gauss Legendre integration $V_0 = \frac{1}{2\pi} \int_0^{2\pi} V(x - \alpha_0 \cos \tau) d\tau$. Where $V(x)$ can be any arbitrary potential which can be analytically defined.

The corresponding momentum basis function is obtained by Fourier transforming position space basis function.

$$\begin{aligned}
 \phi_n(p) &= \frac{1}{\sqrt{2\pi}} \int_{-L/2}^{L/2} e^{-ipx} \phi_n(x) dx \\
 &= \frac{2\sin[L/2((2n\pi/L) - p)]}{\sqrt{2\pi L}((2n\pi/L) - p)}
 \end{aligned}$$

The following equation are representation of one dimensional Xenon potential [1]

$$V(x) = -0.64e^{-0.1424x.^2} \quad (3.34)$$

Figure 3.17 shows energy levels in free field conditions i.e. at α_0 . There are three bound states out which two are perfectly bound and the third one is very close to continuum. Figure 3.18 shows how first few state energies vary as we increase α_0 . In contrast to morse potential, the number of bound state are increasing as we are increasing the AC field parameter.

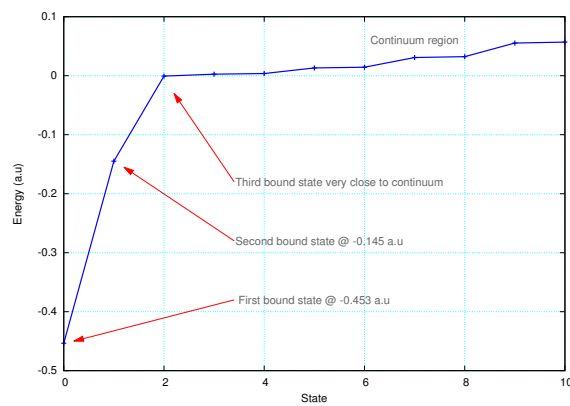


FIGURE 3.17: Energy levels for xenon model potential depicting two perfectly bound states.

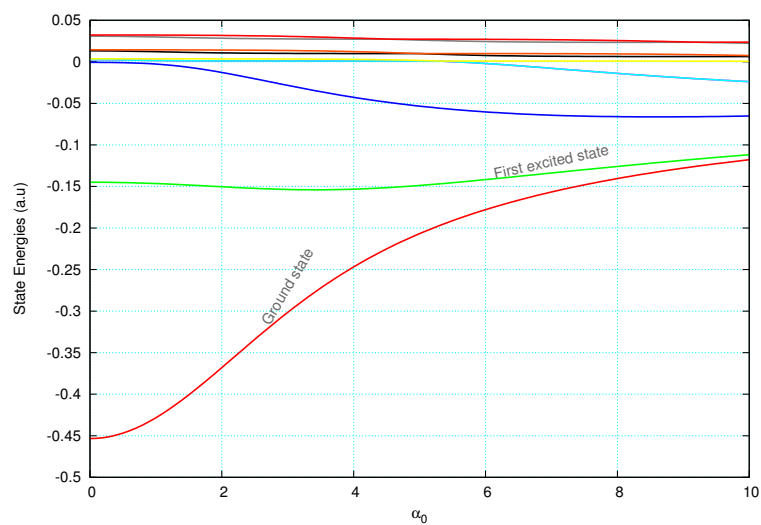


FIGURE 3.18: The two bound states Energies for xenon model potential as as a function of α_0 .

The following Fig 3.19 and 3.20 shows probability density plot in both spaces for the first two states w.r.t α_0 . In the earlier section S_ρ was increasing with α_0 and position space densities are localized in two potential wells with increasing α_0 , which is now supported by broad distribution in position space while increasing α_0 . S_γ was decreasing with α_0 , which is also supported by sharp distribution in momentum space with α_0 in Fig 3.21 and 3.22.

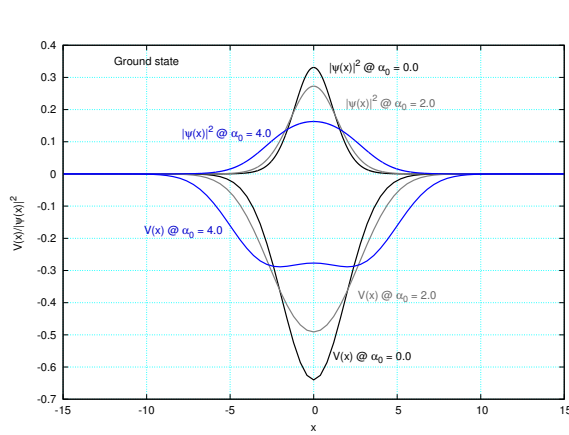


FIGURE 3.19: Xenon model potential and Probability densities for Ground state in position space as function of α_0

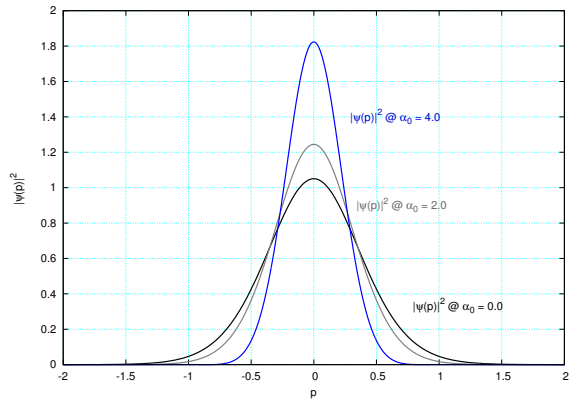


FIGURE 3.21: The corresponding Probability densities for Ground state in momentum space as function of α_0

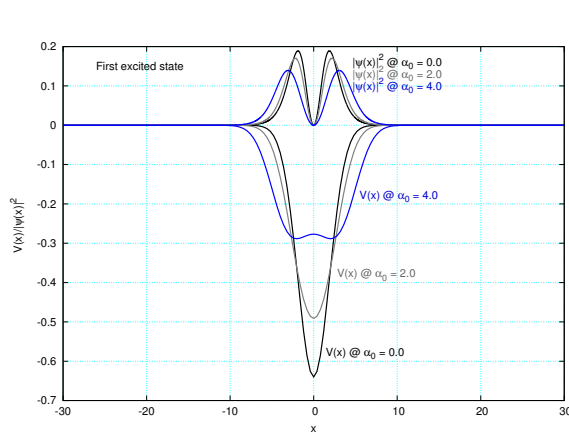


FIGURE 3.20: Xenon model potential and Probability densities for First excited state in position space as function of α_0

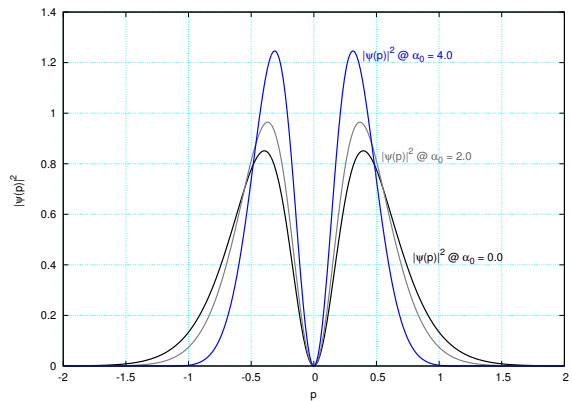


FIGURE 3.22: The corresponding Probability densities for First excited state in momentum space as function of α_0

Figure 3.23, 3.24 shows how S_ρ , S_γ and $S_\rho + S_\gamma$ for ground and the first excited state vary with α_0 . For both states S_ρ is increasing with α_0 and S_γ is decreasing with α_0 . In Fig 3.23 the smaller plot show, how $S_\rho + S_\gamma$ vary with α_0 in a smaller range. For this case, one can clearly see that $S_\rho + S_\gamma$ goes through a minimum while increasing α_0 .

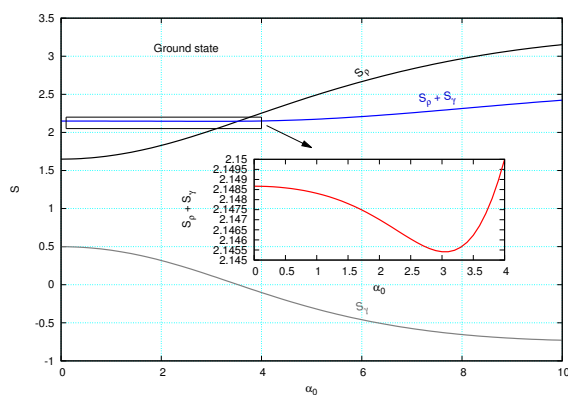


FIGURE 3.23: Ground state Information entropies as a function of α_0

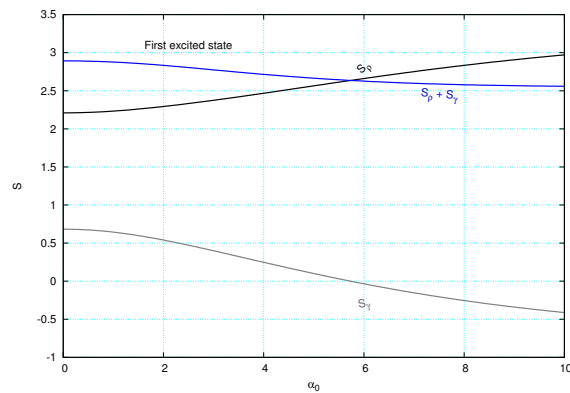


FIGURE 3.24: First excited state Information entropies as a function of α_0

For Xenon potential, a careful calculations is required to be done beyond $\alpha_0 > 5.0$ a.u.

REFERENCES

- [1] A. Fleischer, V. Averbukh, and N. Moiseyev, Phys. Rev. A 69, 043404 (2004).
- [2] "www.octave.org"
- [3] GNU Octave Manual by Jhon W. Eaton.